Supplementary Information

Improved efficiency of inverted planar perovskite solar cells with ultrahigh work function doped polymer as alternative hole transport layer

Gailan A. Al-Dainy[a],*, Zeid N. Al Sudani[a], Ahmed Hashoosh[a], Fumiya Watanabe[a], Alexandru S. Biris[a],*, and Shawn E. Bourdo[a],*

[a] Center for Integrative Nanotechnology Sciences, University of Arkansas at Little Rock, 2801 S. University Ave., Little Rock, AR, 72204 (USA).
*Corresponding Authors: gaaldainy@ualr.edu, gaaldainy@gmail.com (GA Al-Dainy), sxbourdo@ualr.edu (S. E. Bourdo).

Experimental Details.

1. Materials and methods

Unless stated otherwise, all materials in this study were purchased from Sigma-Aldrich and used as received. Lead (II) iodide, 99.9985% (metals basis), was purchased from Alfa Aesar, S-P3MEET solutions were provided by Plextronics, Inc Plexcore® PV 1000, Sigma Aldrich RG-1155. Dimethyl sulfoxide, anhydrous, ≥99.9%, was obtained from Sigma-Aldrich, and chlorobenzene, 99.8%, extra dry, was obtained from Acros. PFI was obtained from Sigma Aldrich (Nafion 117- solution) as a 5 wt% dispersion in a mixed solvent of 45 vol% water and 55 vol% lower aliphatic alcohols.

- **Doping S-P3MEET polymer with PFI**

To dope S-P3MEET (Plexcore ® OC RG-1155) with PFI, the blended solutions were prepared by mixing pure solutions of S-P3MEET and PFI in an appropriate ratio. The blended solutions were stirred and stored at room temperature (RT). The desired ratios of PFI in S-P3MEET were 5 wt%,10wt%, and 15wt%. To increase the wettability of the triple-cation perovskite precursor solution onto fluorinated S-P3MEET substrate, the blended solution of S-P3MEET and PFI was diluted with a mixture of deionized water (10%) and isopropyl alcohol (30%)[1]. To avoid the larger agglomerate particles present in the PFI and S-P3MEET blended solution, we freshly prepared and deposited the fluorinated S-P3MEET blend solution after 3 hours of stirring[2].

- **Triple-cation perovskite precursor solution**

To prepare the triple-cation CsFAMA perovskite precursor solution, we followed our previous procedure[3], in which 960 µL of mixed perovskite solution was first prepared by dissolving FAI (1M), PbI_2 (1.1 M), MABr (0.2 M), and $PbBr_2$ (0.2 M) in an anhydrous co-solvent of DMF : DMSO (4 : 1 by volume, Acros). Then, a 40-µL stock solution of CsI (1.5 M) in DMSO was added to the mixed perovskite to achieve the desired triple cation composition. The stock solutions of inorganic parts (PbI_2, $PbBr_2$, and CsI) were placed on a hotplate at room temperature (RT) and stirred at

150ºC for 15 min. After that, the stock solutions were left to cool to RT. To get single-cation perovskite of $FAPbI_3$ and/or $MAPbBr_3$, the completely dissolved stock solutions of PbI_2 and $PbBr_2$ were mixed with the organic powder (FAI and MABr) at desired volume and then further stirred for 5-6 hours at RT. To get the final concentration solution of the nominal composition $[Cs_{0.04}(MA_{0.17}FA_{0.83})_{0.96}\ Pb(I_{0.83}Br_{0.17})_3]$ perovskite labeled as CsMAFA, a mixed solution of $FAPbI_3$ and $MAPbBr_3$ referred to as MAFA was further mixed with 4% of CsI. The final precursor solution of triple cation with nominal composition of 0.04 CsI and 0.96 MAFA was fourth stirred at RT for 12 hours to get a completely mixed solution for aging the precursor solution[4].

1. Perovskite solar cell fabrication

Similarly, to our previous work[3,5], the pre-patterned indium tin oxide (ITO)- glass substrates with a sheet resistance of 20Ω·s·q−1 - Ossila was cleaned by sonication in 1% Hellmanex water solution for 10 min. After rinsing with deionized water, the substrates were sonicated again in isopropyl alcohol (IPA) for 15 min. They were then dried with compressed nitrogen gas flow and stored in a vacuum oven overnight at 35°C to remove all the moisture from their surface. The last traces of organic residues were further cleaned by ozone-ultraviolet treatment for 10 min. The solutions of undoped and doped SP3MEET were spin-coated onto ITO at different speeds to obtain the same film thickness. After that, the films were annealed on a hotplate at 110°C for 15 min. The HTL of PEDOT:PSS (Al 4083 - Osslila) was spin-coated onto ITO and then annealed on a hotplate at 120°C for 20 min. All the HTLs were deposited in ambient air with relative humidity less than 40%. Afterward, the HTL substrates were transferred to another nitrogen-filled glove box (zero PPM of oxygen and moisture) to deposit the triple-cation perovskite layer. The perovskite $Cs_{0.04}(MA_{0.17}FA_{0.83})_{0.96}\ Pb(I_{0.83}Br_{0.17})_3$ solution was spin coated in one step at 4000 rpm for 30s. During the first 10 seconds of spinning program, 100 µL of [(FAI+MABr)/ IPA] was dropped onto the spinning substrate within a short time (less than 2 seconds). Thereafter, the films were annealed at 100°C for 60 min in a nitrogen-filled glovebox (zero PPM of oxygen and moisture). After the perovskite annealing process, the substrates were cooled down for few minutes, and an electron transport layer (ETL) of $PC_{60}BM$ (20 mg/mL) in chlorobenzene (CB) was spin-coated onto the perovskite at 2000 rpm for 30s, and, sequentially, an interface layer of bathocuproine (BCP, 0.5 mg/mL in anhydrous ethanol- Acros) was spin-coated onto the ETL at 6000 rpm for 15s. After that, the devices were wiped from side of cathode strip using a cotton swab wetted in anhydrous mixed solvent of DMF: CB (1: 6 by volume). The devices were aged one day before silver electrode thermal deposition to evaporate the solvents from the device's layers. Finally, a 100-nm-thick silver electrode was evaporated using an Angstrom thermal evaporator at 10^{-6} Torr, deposited at a rate of 0.1 Å/s, and, after a 4-nm-thick electrode was achieved, the deposition rate was increased up 1.2 Å/s. For device encapsulation, one drop of UV-curable epoxy (E131, Ossila Ltd.) was dropped onto the center of the device, then a glass slide (C181, Ossila Ltd.) was placed onto the epoxy droplet. Finally, the epoxy was cured under a UV light source for 25 min.

2. Perovskite solar cell characterization

The PSC devices were characterized based on our previously reported method[3,5]. Devices were analyzed in ambient conditions (70% RH ± 5%), and the current–voltage (J-V) measurements were taken under 1.5 AM sunlight simulator with incident light power of 100 $mW \cdot cm^{-2}$ (PV Measurements, Inc.). An NREL-certified silicon reference cell was utilized to calibrate the integrated light output from the simulator to 100 mW cm^{-2} at 25°C, and a Keithley 2400 source meter was utilized for electrical measurements. An aperture mask (0.0256 cm^2) was put over each

solar cell to accurately define the device area and minimize absorption of stray light. LabView software was used to sweep voltages from -1 to +1.2 V for forward scan and from +1.2 to -1 V for reverse scan at a rate of 0.4 V/s, then Igor software was used to analyze the J-V curve. External quantum efficiency measurements were performed using a spectral-responsivity system (Bentham model PVE 300). The lifetime of the devices' measurements was carried out on best-performing cells without encapsulation. The devices were tested in ambient conditions at relative humidity (RH) conditions (50-75%), and they were stored in the dark by covering with aluminum foil during storing time.

3. Perovskite device's layer characterization.

- **Steady-state photoluminescence (PL) spectra**.

The steady-state PL spectra were obtained with a photoluminescence spectrophotometer (R928P, TCSPC-Flormax Horiba). The CsFAMA perovskite was deposited onto the HTLs/quartz with mixed organic halide in IPA anti-solvent treatment. PL spectra were recorded at RT by exciting the perovskite films at 460 nm with a standard 450-W Xenon CW lamp with wavelength range from 630 nm to 850 nm. The samples were mounted at 60° and the emission recorded at 90° from the incident beam path.

- **Conductivity and space charge-limited-current measurement**

To measure the conductivity and mobility of the HTL films, glass/ITO/HTLs/Ag devices with 0.12 cm^2 active area were fabricated. The data were collected using two mechanical probes and Keithley 2400 sourcemeter. The voltage was swept from -1 to +1 V and from 2 to 7 V for conductivity and mobility measurements, respectively. Then, according to the space charge-limited-current (SCLC), the data was analyzed.

- **Surface topography and device film thickness measurements**

An AFM (Bruker Dimension 3100 Icon Fast Scan) was used to measure surface morphology and film thickness. The tapping mode was applied with a 1-Hz scan rate and different scan sizes. The data of the scanned surface were collected using a silicon tip connected to a cantilever with 300 KHz resonance frequency and 40 N/m force constant. For thickness measurements, the HTL films were wiped with a wet acetone cotton swab to get a highly sharp edge at the glass-film interface, then NanoScope Analysis (ver.1.5-Bruker) was utilized for image analyses. All AFM measurements were taken at room temperature, with the microscope housed in an acoustic/vibration isolation hood to protect it from any acoustic/vibrational noise.

- **Scanning electron microscopy (SEM) for PSC measurements**

To study the surface topography of the perovskite films and a cross-section of the device layers, SEM (JEOL JSM 7000F) was used. For the perovskite topography measurement, films were deposited onto the HTL/glass substrate. The cross-section of the PSC device was measured by breaking the whole device in the middle by pressing with running pliers. This was then mounted vertically onto an aluminum stub with double-sided carbon tape and loaded into the SEM stage. For grain size analysis of the perovskite films and thickness estimate of the whole PSC device, ImageJ software was used.

- **Kelvin probe force microscopy measurements (KPFM)**

To measure the electronic properties of the PSC device layers by KPFM, the films were deposited on the ITO/glass substrate, which was then grounded onto the AFM stage with silver paste to reduce error signal and charge build-up phenomena. The measurements were performed in ambient conditions, and the surface potential was measured at four random surface spots for each sample to rule out the effects of surface contamination or defects. The measurements were carried out using a Bruker SCM-PIT-V2 electrically conductive probe made of antimony (n) -doped silicon with ~0.01-0.025 Ω cm resistivity and 25-nm tip radius. The cantilever was coated with platinum-iridium on the back side, with a nominal spring constant of 3-6 N/m and a resonant frequency of 75 KH. A freshly cleaved sample of highly oriented pyrolytic graphite (HOPG) was used for tip calibration. The dual-pass amplitude modulation of the KPFM was used for surface potential measurements. The distance between the tip and the sample (lift scan height) was maintained to be 50 nm with 1000 mV sample biased to get decent images.

- **X-ray photoelectron spectroscopy (XPS) measurements**

The elemental composition of the perovskite films was analyzed using an x-ray photoelectron spectrometer (K-Alpha, Thermo Scientific, Waltham, MA) with a monochromatic Al Kα ($h\upsilon$ = 1436.6 eV) x-ray source. The x-ray power was 36 W, and the beam size was 400 μm in diameter. Survey and/or narrow scans were done on each sample at a pass energy (CAE) of 200 eV and 1 eV step size. Etching the surface of the samples was done at 60 seconds to evaluate the elements in the bulk. Then, Avantage software was used to analyze the obtained spectra.

- **Surface energy of the HTLs**

To study the surface energy of the HTLs, the contact angle of water drops on the HTLs was measured using an EasyDrop (DSA1) system (Kruss Co.) with sessile drop method. To measure the contact angle of the surface, 5 μL of deionized water were dispensed gently via computer-controlled syringe at different locations on the surface of the films/ITO/glass substrates, then a CCD camera was used to capture images of the droplets on the surface. The measurement was performed in ambient conditions at room temperature.

- **Optical properties of the PSCs layers**

To study the optical properties of the HTLs and perovskite active layer, transmittance and absorption spectra were recorded by UV-VIS-NIR spectroscopy (Shimatzu-3600) at wavelengths ranging from 300-1000 nm.

- **Chemical structure of the HTLs**

The chemical structure of the S-P3MEET, PFI, and PEDOT:PSS were drawn and edited using HTML5/JavaScript implementation of ***ChemDraw JS***.

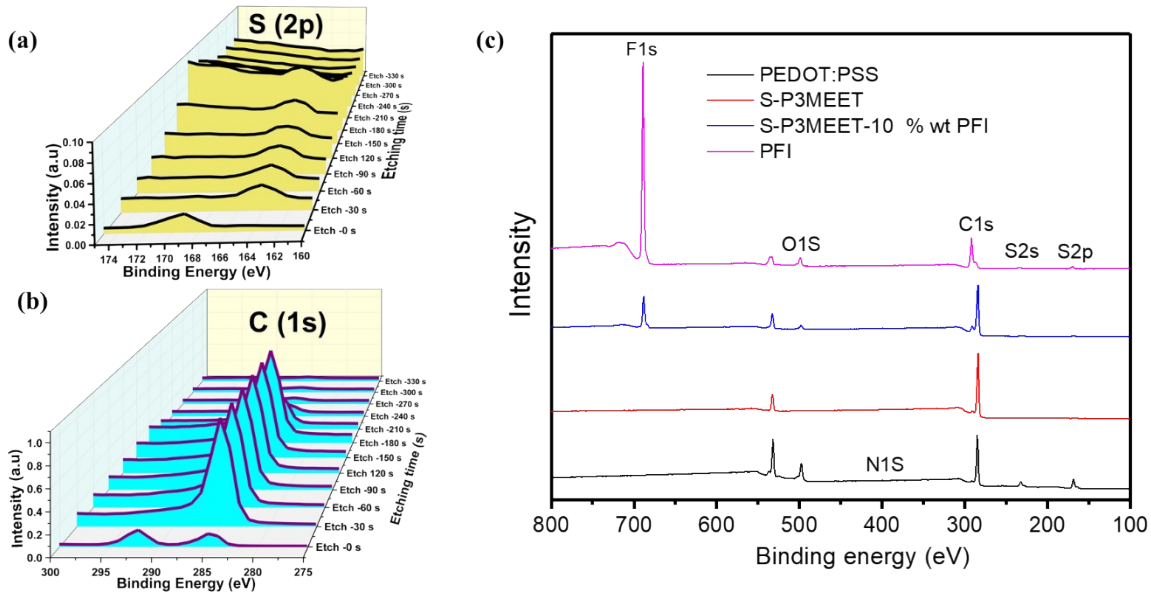

Figure S1. XPS depth profiling of the S-P3MEET-PFI-10% wt film with etching times of 0-330 s for: (a) S(2p) core-level spectra and (b) C(1S) core-level spectra. (c) Overview spectra XPS survey scan of the pristine S-P3MEET, PFI, fluorinated S-P3MEET, and PEDOT:PSS samples.

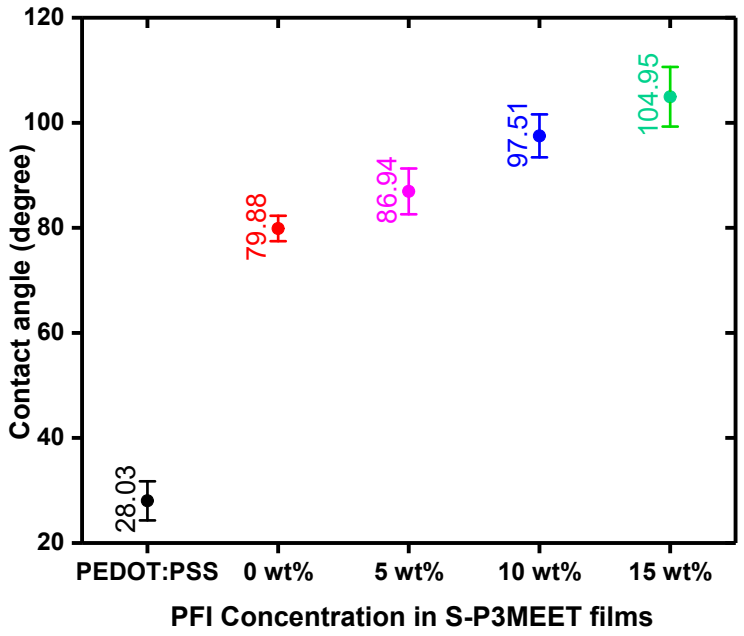

Figure S2. The mean water contact angle values (whiskers and standard deviation) of the HTLs/ITO/glass film surface; for n=10 images displayed.

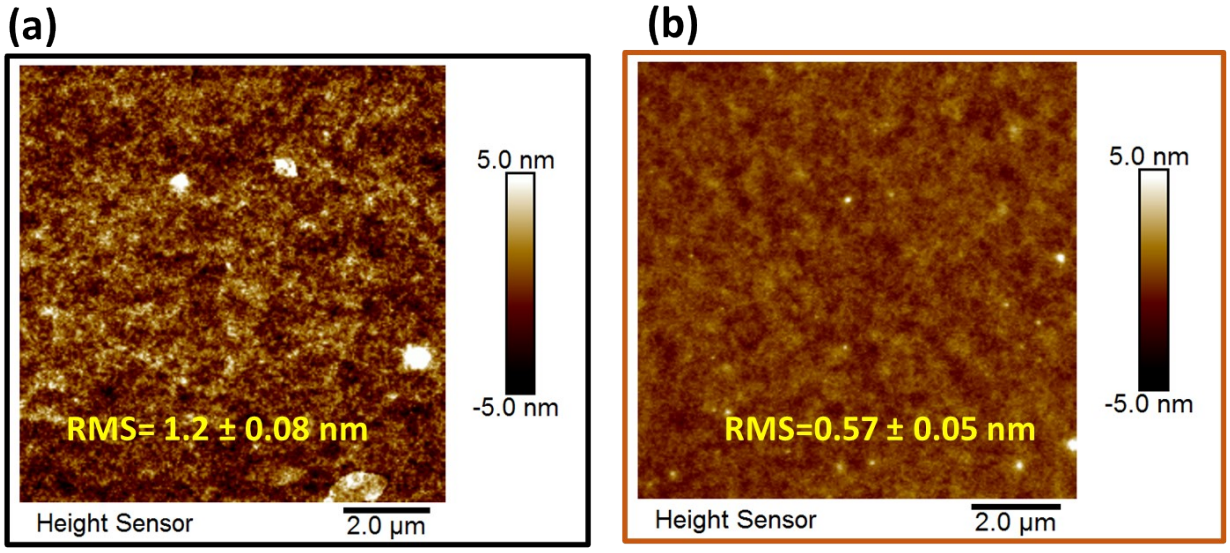

Figure S3. AFM morphology of (a) FPEDOT:PSS and (b) PFI. All the films were deposited onto glass substrates.

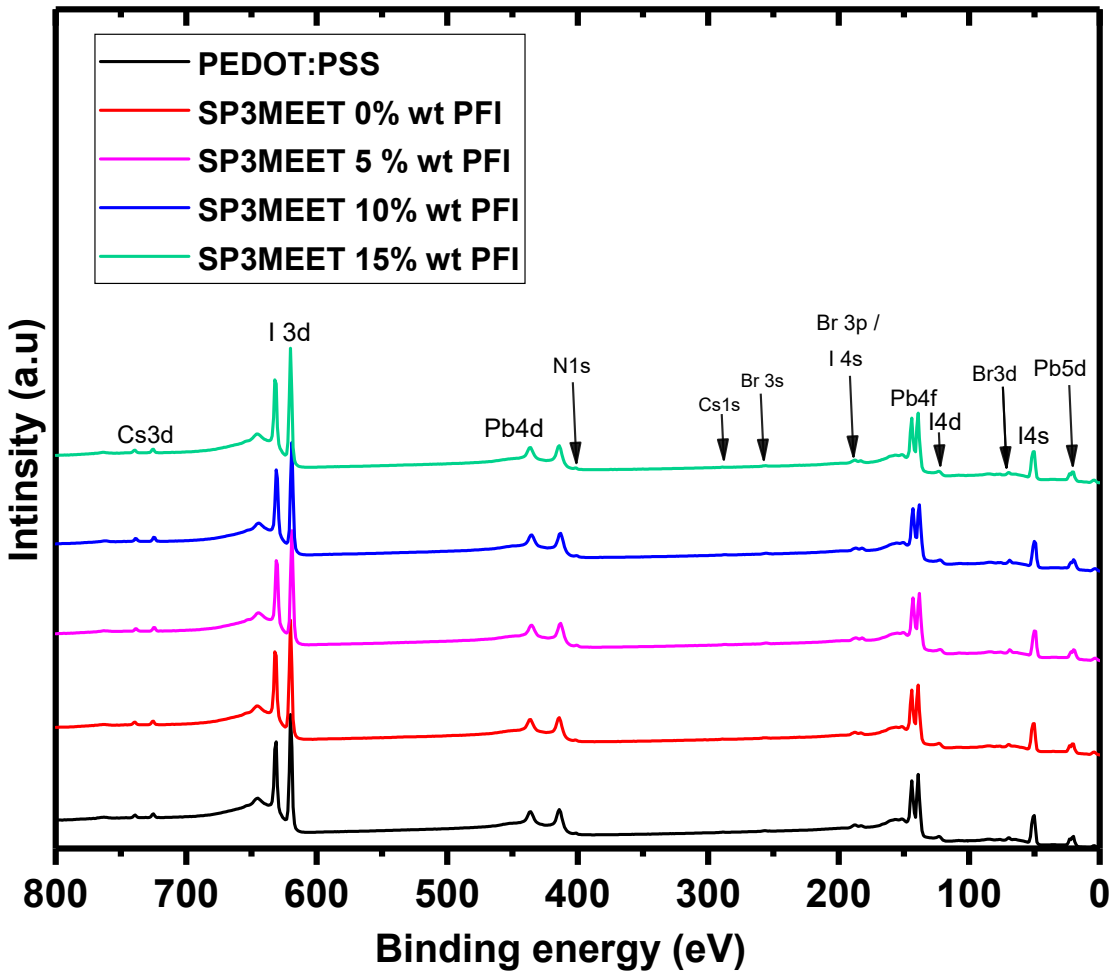

Figure S4. Overview spectra XPS survey scan of the CsMAFA perovskite deposited onto the different HTLs.

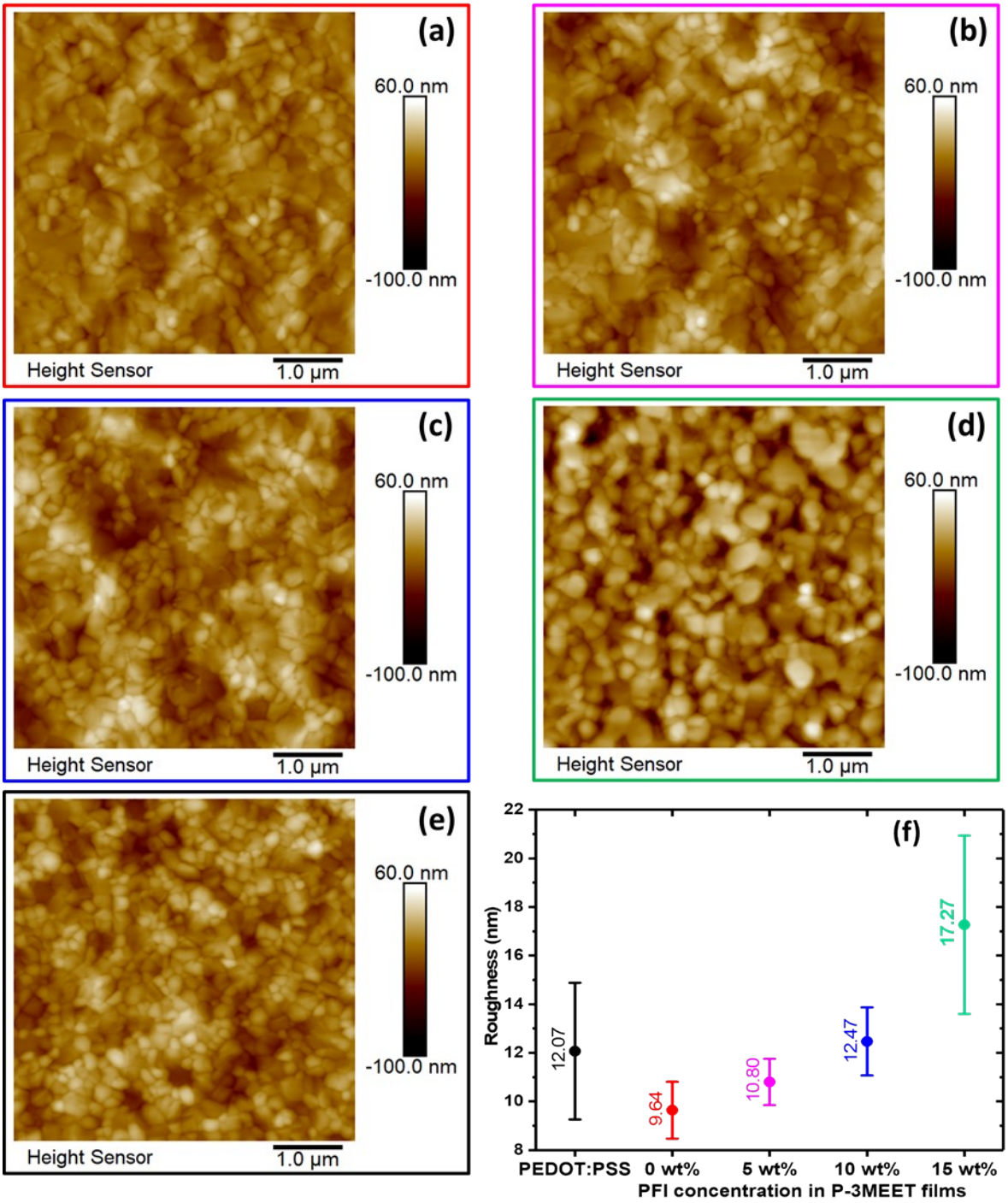

Figure S5. AFM morphology images of $Cs_{0.04}(FA_{0.83}MA_{0.17})_{0.95}Pb(I_{0.83}Br_{0.17})_3$ perovskite films deposited onto (a) pristine S-P3MEET, (b) S-P3MEET- 5% wt PFI, (c) S-P3MEET- 10% wt PFI, (d) S-P3MEET- 15% wt PFI, and (e) FPEDOT:PSS films. (f) The mean values (whiskers are standard deviation) of perovskite film roughness determined from AFM images (n=4).

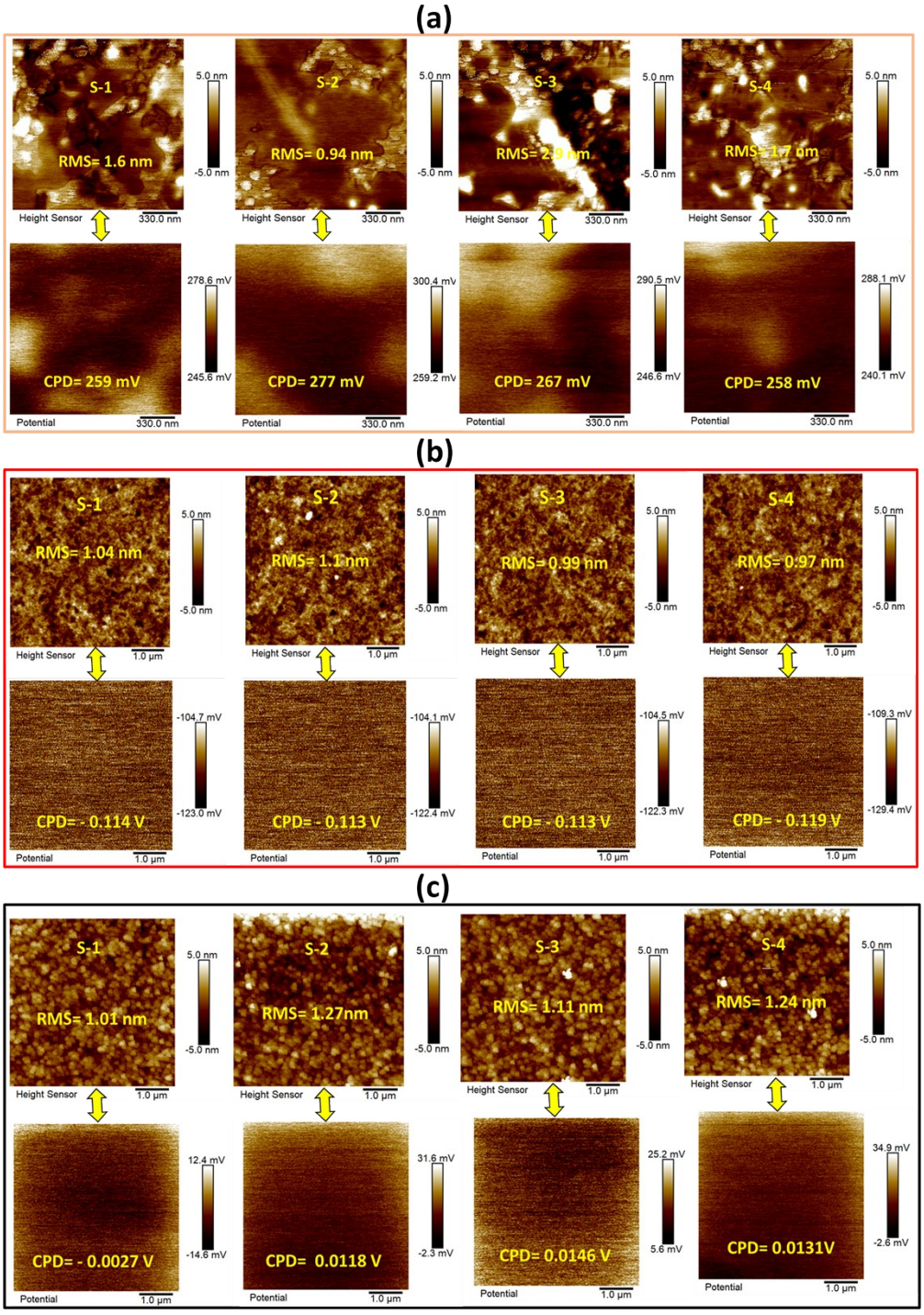

Figure S6. Morphology and CPD mapping of 4 spots on (a) HOPG sample, (b) pristine S-P3MEET, and (c) PEDOT:PSS.

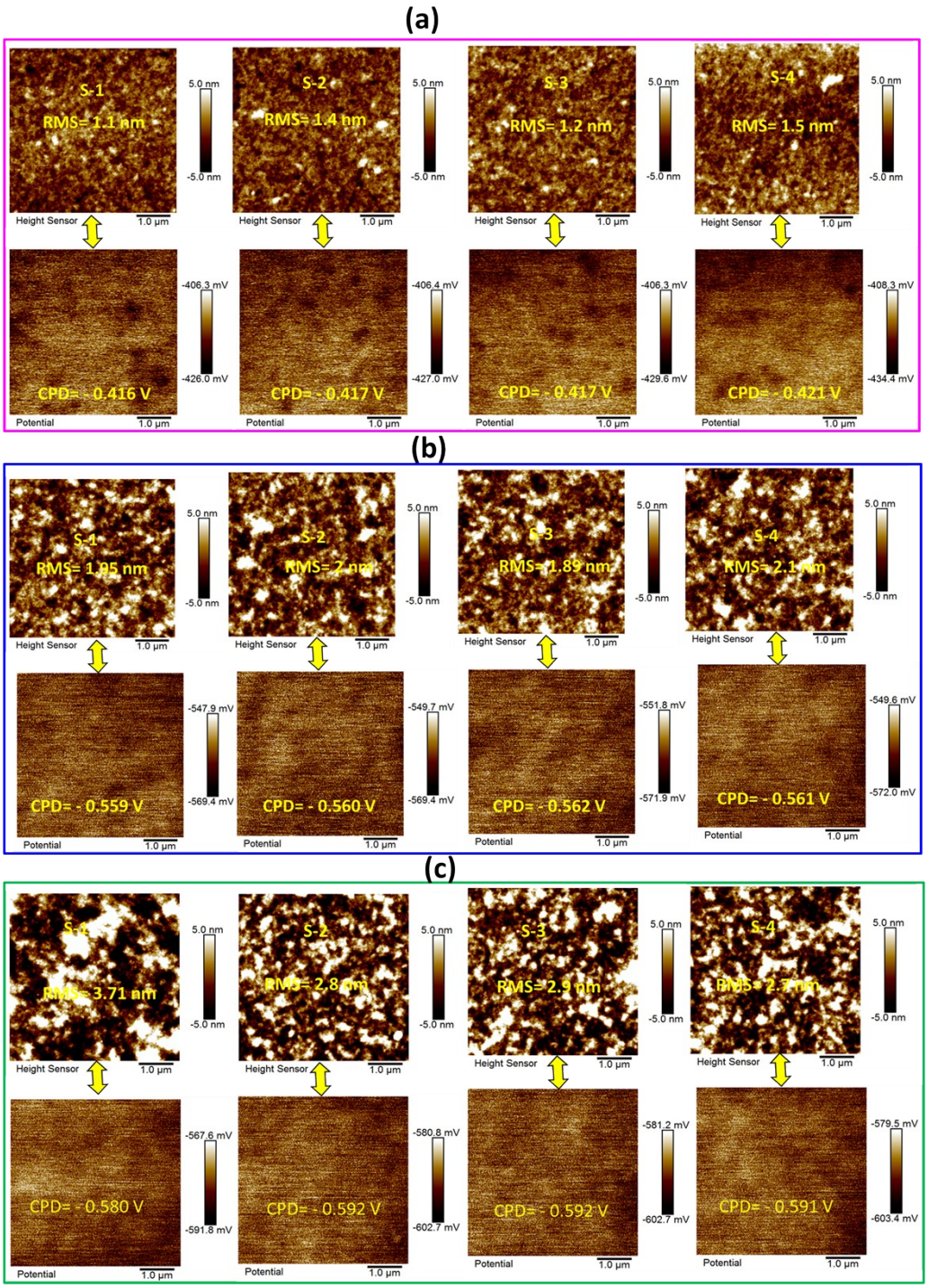

Figure S7. Morphology and CPD mapping of 4 spots on (a) S-P3MEET- 5% wt PFI, (b) S-P3MEET- 10% wt PFI, and (c) S-P3MEET- 15% wt PFI.

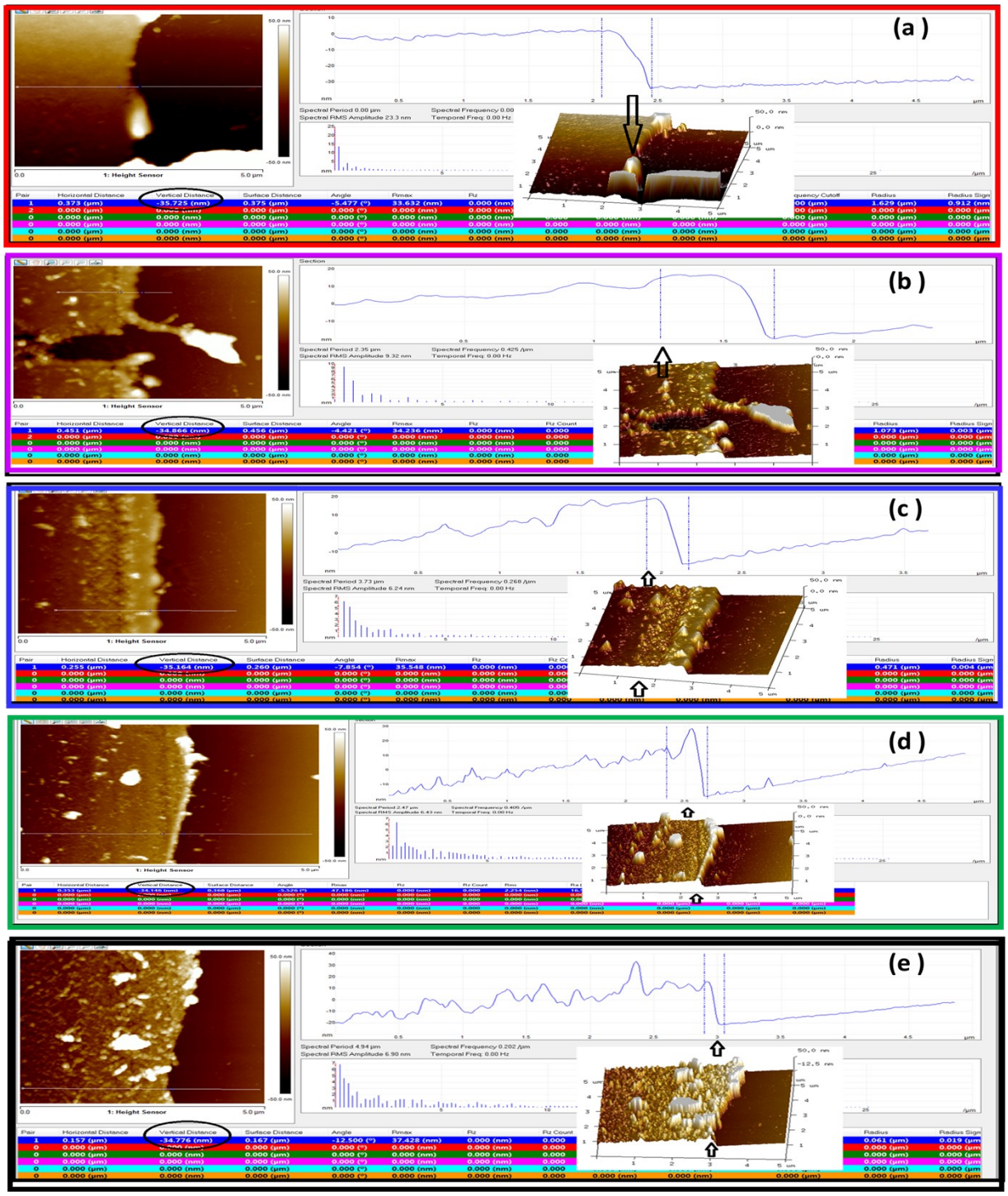

Figure S8. Thickness measurements of HTLs by AFM: (a) pristine S-P3MEET, (b) S-P3MEET-5% wt PFI, (c) S-P3MEET- 10% wt PFI, (d) S-P3MEET- 15% wt PFI, and (e) FPEDOT:PSS films. Here, all the films have thickness about 35±1 nm.

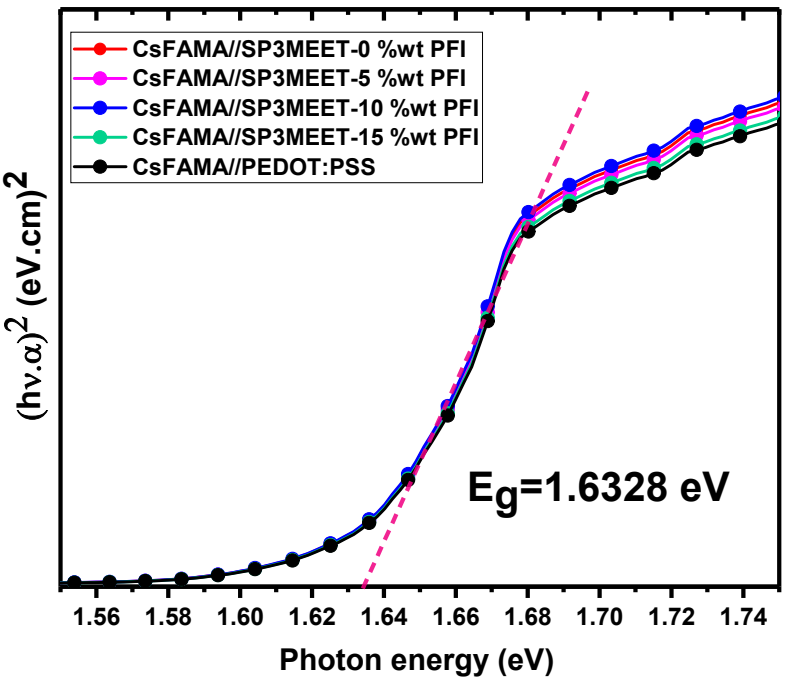

Figure S9. Optical band gap (E_g) of $Cs_{0.04}(FA_{0.83}MA_{0.17})_{0.95}Pb(I_{0.83}Br_{0.17})_3$ perovskite films prepared with (FAI+MABr)/IPA treatment and deposited onto different HTLs/ITO.

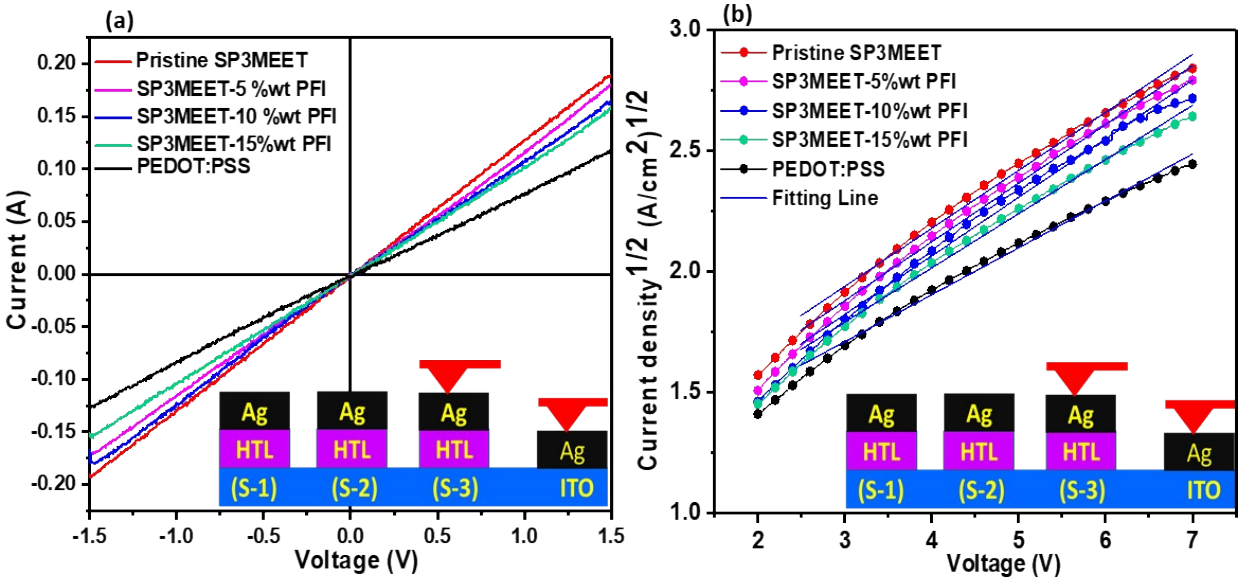

Figure S10. (a) Current-voltage (I–V) characteristics for ITO/HTLs/Ag devices and (b) the space-charge-limited current (SCLC) region J–V^2 characteristics for ITO/HTLs/Ag devices. Here, the raw data for each curve presented in (a) and (b) is the average of three spots selected for each type of sample (S-1, S-2, and S-3), as shown in the insert of (a) and (b).

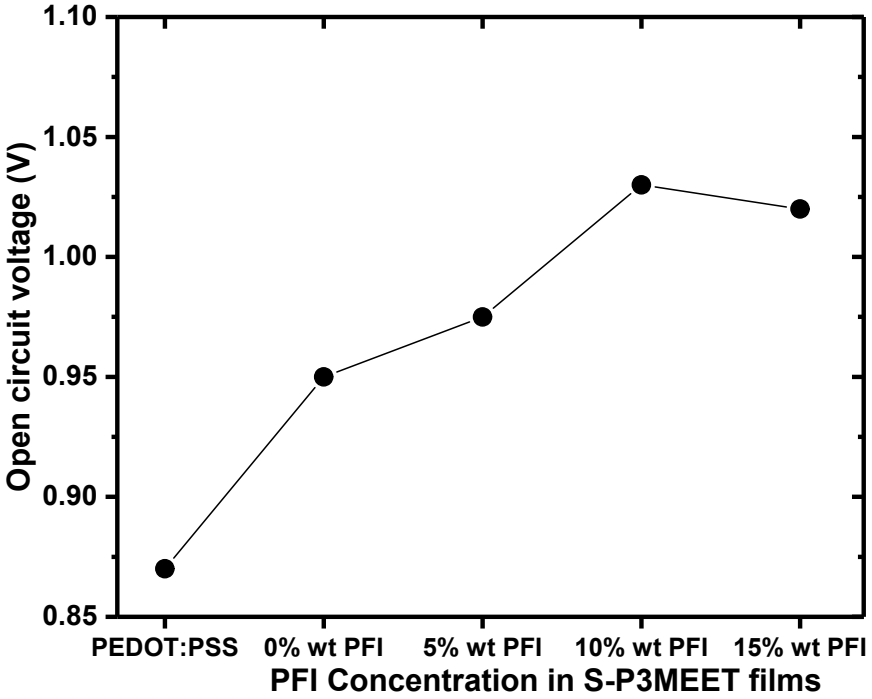

Figure S11. The average open circuit voltage of perovskite solar cells, based on 42 devices total, versus the various WF of HTLs.

Table S1. Summary of reported superior triple-cation PSC performances in both inverted planar (p-i-n) and mesoporous (n-i-p) configurations. The inverted planar devices based on fluorinated S-P3MEET exhibit an optimized interface HTL for the highest performance, even higher than some both mesoporous (n-i-p) and inverted architectures.

Structure	J_{sc} mA.cm^{-2}	V_{oc} (V)	FF (%)	PCE (%)	References (Ref)
(p-i-n)	23.50	1.140	80.00	21.40	Ref [6]
(p-i-n)	21.47	0.940	72.00	15.42	Ref [7]
(n-i-p)	23.90	1.150	77.00	21.10	Ref [8]
(n-i-p)	22.50	1.110	78.00	19.40	Ref [9]
(p-i-n)	21.95	1.081	78.40	18.21	Ref [10]
(n-i-p)	21.90	1.073	74.20	17.35	Ref [11]
(p-i-n)	22.87	1.110	70.00	17.75	Ref [12]
(p-i-n)	22.92	1.060	70.27	17.02	Ref [13]
(p-i-n)	22.20	1.070	79.80	18.80	Ref [14]
(n-i-p)	22.54	1.110	72.20	18.07	Ref [15]
(n-i-p)	22.76	1.090	80.63	20.11	Ref [16]
(p-i-n)	24.10	1.170	81.60	23.00	Ref [17]
(n-i-p)	23.30	1.150	73.00	19.50	Ref [18]
(n-i-p)	24.47	1.130	69.36	19.22	Ref [19]
(n-i-p)	24.19	1.047	68.13	17.25	Ref [20]
(p-i-n)	24.4	1.17	81.9	23.3	Ref [21]
(p-i-n)	23.61	1.070	78.00	19.60	**This work**

References

1 F. Paquin, J. Rivnay, A. Salleo, N. Stingelin and C. Silva, *J. Mater. Chem. C*, 2015, **3**, 10715–10722.

2 S. A. Mauger and A. J. Moulé, *Org. Electron.*, 2011, **12**, 1948–1956.

3 G. Al-Dainy, F. Watanabe, A. S. Biris and S. E. Bourdo, *ACS Appl. Energy Mater.*, 2021, **4**, 3297–3309.

4 P. Boonmongkolras, D. Kim, E. M. Alhabshi, I. Gereige and B. Shin, *RSC Adv.*, 2018, **8**, 21551–21557.

5 G. A. Al-Dainy, F. Watanabe, G. K. Kannarpady, A. Ghosh, B. Berry, A. S. Biris and S. E. Bourdo, *ACS Omega*, 2020, **5**, 1887–1901.

6 A. Ng, Z. Ren, H. Hu, P. W. K. Fong, Q. Shen, S. H. Cheung, P. Qin, J. W. Lee, A. B. Djurišić, S. K. So, G. Li, Y. Yang and C. Surya, *Adv. Mater.*, 2018, **30**, 1–10.

7 K. Lee, H. Yu, J. W. Lee, J. Oh, S. Bae, S. K. Kim and J. Jang, *J. Mater. Chem. C*, 2018, **6**, 6250–6256.

8 T. Singh, S. Öz, A. Sasinska, R. Frohnhoven, S. Mathur and T. Miyasaka, *Adv. Funct. Mater.*, , DOI:10.1002/adfm.201706287.

9 J. E. Bishop, C. D. Read, J. A. Smith, T. J. Routledge and D. G. Lidzey, *Sci. Rep.*, 2020, **10**, 1–8.

10 Y. Wu, X. Yang, W. Chen, Y. Yue, M. Cai, F. Xie, E. Bi, A. Islam and L. Han, *Nat. Energy*, , DOI:10.1038/nenergy.2016.148.

11 C. Yi, J. Luo, S. Meloni, A. Boziki, N. Ashari-Astani, C. Grätzel, S. M. Zakeeruddin, U. Röthlisberger and M. Grätzel, *Energy Environ. Sci.*, 2016, **9**, 656–662.

12 U. K. Thakur, P. Kumar, S. Gusarov, A. E. Kobryn, S. Riddell, A. Goswami, K. M. Alam, S. Savela, P. Kar, T. Thundat, A. Meldrum and K. Shankar, *ACS Appl. Mater. Interfaces*, 2020, **12**, 11467–11478.

13 N. Kumar, H. B. Lee, S. Hwang and J. W. Kang, *J. Mater. Chem. A*, 2020, **8**, 3357–3368.

14 M. Stolterfoht, C. M. Wolff, Y. Amir, A. Paulke, L.Perdigón-Toro, P. Caprioglio and D. Neher., Energy Environ. Sci., 2017,10, 1530-1539

15 R. Singh, S. Sandhu, H. Yadav and J. J. Lee, *ACS Appl. Mater. Interfaces*, 2019, **11**, 29941–29949.

16 G. Xia, B. Huang, Y. Zhang, X. Zhao, C. Wang, C. Jia, J. Zhao, W. Chen and J. Li, *Adv. Mater.*, 2019, **31**, 1–9.

17 X. Zheng, Y. Hou, C. Bao, J. Yin, F. Yuan, Z. Huang, K. Song, J. Liu, J. Troughton, N. Gasparini, C. Zhou, Y. Lin, D. J. Xue, B. Chen, A. K. Johnston, N. Wei, M. N. Hedhili, M. Wei, A. Y. Alsalloum, P. Maity, B. Turedi, C. Yang, D. Baran, T. D. Anthopoulos, Y. Han, Z. H. Lu, O. F. Mohammed, F. Gao, E. H. Sargent and O. M. Bakr, *Nat. Energy*, 2020, **5**, 131–140.

18 T. Ye, M. Petrovic, S. Peng, J. L. K. Yoong, C. Vijila and S. Ramakrishna, *ACS Appl. Mater. Interfaces*, 2017, **9**, 2358–2368.

19 Y. Wang, J. Wu, P. Zhang, D. Liu, T. Zhang, L. Ji, X. Gu, Z. David Chen and S. Li, *Nano Energy*, 2017, **39**, 616–625.

20 A. Huang, L. Lei, J. Zhu, Y. Yu, Y. Liu, S. Yang, S. Bao, X. Cao and P. Jin, *ACS Appl. Mater. Interfaces*, 2017, **9**, 2016–2022.

21 H. Zhou, L. Wang, N. Li, Y. Zhang, L. Chen, X. Ke, Z. Chen, Z. Wang, M. Sui, Y. Chen, Y. Huang, L. Liang, Z. Xu, Q. Chen, L.-D. Sun and C.-H. Yan, *J. Mater. Chem. A*, 2020 ,**8**, 14106-14113